Article

Real-Scale Integral Valorization of Waste Orange Peel via Hydrodynamic Cavitation

Francesco Meneguzzo [1,*], Cecilia Brunetti [2], Alexandra Fidalgo [3], Rosaria Ciriminna [4], Riccardo Delisi [5], Lorenzo Albanese [6], Federica Zabini [7], Antonella Gori [8], Luana Beatriz dos Santos Nascimento [9], Anna De Carlo [10], Francesco Ferrini [11], Laura M. Ilharco [12], Mario Pagliaro [13]

[1] Institute for Bioeconomy, National Research Council, 10 Via Madonna del Piano, I-50019 Sesto Fiorentino (FI), Italy; francesco.meneguzzo@cnr.it
[2] Institute for Bioeconomy, National Research Council, 10 Via Madonna del Piano, I-50019 Sesto Fiorentino (FI), Italy; cecilia.brunetti@cnr.it
[3] Centro de Química-Física Molecular and IN-Institute of Nanoscience and Nanotechnology, Instituto Superior Técnico, University of Lisboa, Complexo I, Avenida Rovisco Pais 1, 1649-004 Lisboa, Portugal; alexandra.m.abrantes.fidalgo@gmail.com
[4] Istituto per lo Studio dei Materiali Nanostrutturati, CNR, via U. La Malfa 153, 90146, Palermo, Italy; rosaria.ciriminna@cnr.it
[5] Renovo Biochemicals srl, Via P. Verri,1 46100 Mantova (MN); riccardo.delisi@renovospa.it
[6] Institute for Bioeconomy, National Research Council, 10 Via Madonna del Piano, I-50019 Sesto Fiorentino (FI), Italy; l.albanese@ibimet.cnr.it
[7] Institute for Bioeconomy, National Research Council, 10 Via Madonna del Piano, I-50019 Sesto Fiorentino (FI), Italy; f.zabini@ibimet.cnr.it
[8] Department of Agriculture, Environment, Food and Forestry (DAGRI), University of Florence, Viale delle Idee 30, I-50019 Sesto Fiorentino (FI), Italy; antonella.gori@unifi.it
[9] Department of Agriculture, Environment, Food and Forestry (DAGRI), University of Florence, Viale delle Idee 30, I-50019 Sesto Fiorentino (FI), Italy; lulibia.17@gmail.com
[10] Institute for Bioeconomy, National Research Council, 10 Via Madonna del Piano, I-50019 Sesto Fiorentino (FI), Italy, and Department of Agriculture, Environment, Food and Forestry (DAGRI), University of Florence, Viale delle Idee 30, I-50019 Sesto Fiorentino (FI); anna.decarlo@cnr.it
[11] Department of Agriculture, Environment, Food and Forestry (DAGRI), University of Florence, Viale delle Idee 30, I-50019 Sesto Fiorentino (FI), Italy; francesco.ferrini@unifi.it
[12] Centro de Química-Física Molecular and IN-Institute of Nanoscience and Nanotechnology, Instituto Superior Técnico, University of Lisboa, Complexo I, Avenida Rovisco Pais 1, 1649-004 Lisboa, Portugal; lilharco@tecnico.ulisboa.pt
[13] Istituto per lo Studio dei Materiali Nanostrutturati, CNR, via U. La Malfa 153, 90146, Palermo, Italy; mario.pagliaro@cnr.it
* Correspondence: francesco.meneguzzo@cnr.it; Tel.: (+39-392-985-0002)

Abstract: Waste orange peel represents a heavy burden for the orange juice industry, estimated in several million tons per year worldwide; nevertheless, this by-product is endowed with valuable bioactive compounds, such as pectin, polyphenols and terpenes. The potential value of the waste orange peel has stimulated the search for extraction processes, alternative or complementary to landfilling or to the integral energy conversion. This study introduces controlled hydrodynamic cavitation processes, as a new route to the integral valorization of this by-product, based on simple equipment, speed, effectiveness and efficiency, scalability, and compliance with green extraction principles. Waste orange peel, in batches of several kg, was processed in more than 100 L of water, absent any other raw materials, in a device comprising a Venturi-shaped cavitation reactor. The extractions of pectin, endowed with a very low degree of esterification, polyphenols (flavanones and hydroxycinnamic acid derivatives), and terpenes (mainly *d*-limonene) were effective and fast (high yield, few min of process time), as well as the biomethane generation potential of the process residues was effectively exploited. The achieved results proved the viability of the proposed route

to the integral valorization of waste orange peel, though wide margins exist for further improvements.

Keywords: biomethane; *d*-limonene; flavanones; food waste; green extraction; hydrodynamic cavitation; orange waste; pectin; polyphenols.

1. Introduction

Accounting for 61% of the world's citrus fruit production [1], the global production of sweet orange (*Citrus sinensis* (L.) Osbeck) in 2017-2018 exceeded 47 million tons, 36% of which (17 million tons) were used for orange juice production [2]. Production for 2018-19 was predicted to grow by another 4.2 million metric tons. A huge amount of by-products, estimated at a level between 50 and 60% of the harvest is comprised of discarded fruits, peels and seeds. Effective technologies to upgrade the value of these said by-products, which have been so far mostly dealt with as waste, are of direct and significant relevance to all orange-growing countries and regions, including Brazil, Florida, India, South Africa, Spain, Turkey and Italy [3]. Waste orange peel (WOP), in particular, contains highly valuable bioproducts such as carbohydrate polymers (cellulose, hemicellulose, and pectin), polyphenols (including naringin and hesperidin), and essential oils (mostly *d*-limonene) [1].

The affordable, large-scale extraction and valorization of these compounds would also result in the size reduction of the relevant waste stream, thus relieving the environmental burden related to the still frequent disposal of the WOP in landfills or saving valuable biocompounds before the energy conversion of the residues. About the energetic valorization of WOP, anaerobic co-digestion – after extraction and removal of *d*-limonene, an inhibitory compound – was assessed as the most environmentally performing [3]; indeed, the latter practice has been increasingly applied in some orange intensive production areas, such as Sicily.

In the last fifteen years, numerous green chemistry processes have been applied to extract the valued components of WOP resulting from the orange juice industry. WOP is a potential source of fat (oleic, linoleic, linolenic, palmitic, and stearic acids, and phytosterols), mono- and disaccharides (glucose, fructose, sucrose), organic acids (especially citric and malic acid, tartaric but also benzoic, oxalic and succinic acids), polysaccharides (cellulose, hemicellulose, and pectin), enzymes (pectinesterase, phosphatase, peroxidase), flavonoids (hesperidin, naringin, narirutin), terpenes (*d*-limonene, linalool, myrcene), and pigments (carotenoids, xanthophylls). Few years ago, solvent-free extraction processes using microwave and ultrasound techniques were successfully applied to obtain essential oils, polyphenols and pectin, through microwave hydrothermal processing [4]. Promising results were achieved by means of solar-driven vapor steam distillation, to obtain valued pectin, terpenes and biophenols [5], as well as by means of a solvent-free process based on microwave distillation, hydrodiffusion and gravity [6].

Generally extracted from the orange peel prior to squeezing via a mechanical process (a jet of water breaking the oil-containing glands), orange essential oil (EO) mostly contains *d*-limonene [7], a monoterpene whose average content in *Citrus sinensis* fruit peels is 3.8 wt% on a dry weight basis [8,9]. This molecule was first used in the 1950s as a bio-solvent, and today *d*-limonene is the main ingredient of numerous bio-based functional products whose demand is rapidly growing [9]. In the early 1990s, its plant anti-fungal and antibacterial properties were first identified [10], leading to the development and utilization of biopesticide formulations in which orange oil, and thus *d*-limonene, was the active ingredient [11]. After the discovery of its natural ozone scavenging properties, in 2005 *d*-limonene was proposed as an effective adjuvant in preventive therapies against asthma [12]. Due to its wide-spectrum of antimicrobial, antioxidant and anti-inflammatory properties, *d*-limonene is now used in many cosmetic and nutraceutical applications, as well as an anti-spoilage additive in food [13].

Currently mostly produced from citrus peels (56% from lemons, 30% from limes, and 13% from oranges), and to a lesser extent (14%) from apple pomace [14], pectin is the most valued natural hydrocolloid [15]. Since the early 2000s, it was established that pectin has various beneficial effects

on health and nutrition as a dietary and prebiotic fiber, with numerous applications in the food, feed, cosmetic, medical and pharmaceutical industries [6,15]. Effectively reducing the interfacial surface tension between the oil and the water phases, pectin is also an excellent emulsifier and emulsion stabilizer [16,17]. Orange-extracted pectin powder was added to an oil-in-water sub-micron size emulsion (20% w/w), the latter prepared with a standard homogenizer and using orange oil), showing substantial stability up to at least 30 days from preparation [16].

To the best of our knowledge, no studies have been reported so far, dealing with the application of the hydrodynamic cavitation (HC) processes to extract the valued components of waste orange peel. This study therefore reports the first results concerning a novel route to valorize WOP based on criteria of effectiveness, reliability, efficiency, and affordability. The starting idea was that waste orange peel contains EOs, water-soluble pectin and polyphenols, which could be transferred to the water phase, where a stable oil-in-water emulsion could be created due to the simultaneous presence of EOs and pectin acting as an emulsifier. All this, by means of HC processes and without additives except water, as elucidated in Section 2.2. After the HC-based extraction process, the liquid phase could be used as such to functionalize foods and beverages, affecting both the nutraceutical properties and the shelf life. The residual WOP solid fraction, mostly comprised of cellulose and hemicellulose, could be effectively used to produce biogas in an anaerobic digester, and the resulting digestate used as a soil amendant or easily converted into biochar or hydrochar [18,19].

Generally achieved via pumping a liquid through one of more constrictions of suitable geometry, such as Venturi tubes and orifice plates, controlled hydrodynamic cavitation results in the generation, growth and collapse of microbubbles due to pressure variations in the liquid flow [20]. The increase in kinetic energy at the constriction occurs at the expense of pressure, leading to the generation of microbubbles and nanobubbles, which subsequently collapse under pressure recovery downstream of the constriction [21]. The violent collapse of the cavitation bubbles results in the generation of localized hot spots endowed with extremely high-energy density [22,23], highly reactive free radicals and turbulence, which can result in the intensification of various physical/chemical phenomena, including wastewater remediation [24–26], preparation of nanoemulsions, biodiesel synthesis, water disinfection, and nanoparticle synthesis [27], and many others.

In recent past, cavitation has emerged as a green extraction technology for natural products, reducing process time and energy consumption, while achieving higher extraction yields, as well as a useful tool for the intensification of food and pharmaceuticals processes [27,28]. The growing variety of applications has also stimulated the development of other promising arrangements, such as based on rotating parts [29], and variants of fixed constrictions, for example based on vortex dynamics [30], which are in the process of proving the respective affordability and straightforward scalability.

Real-scale applications of cavitation are quickly spreading in the food and beverage industry, including the processing of food waste [31]. Again, the HC processing of vegetable raw material, such as grains and hops for beer-brewing [32,33], plant leaves [34], and applied to the extraction of bioactive compounds [29], offers distinctive advantages such as shorter process times, higher energy efficiency, higher yields, and enhanced extraction rates. Quantitatively compared with both conventional techniques and newer ones, including acoustic cavitation sustained by ultrasound irradiation, the performance of HC-based processes was found to be clearly superior due to enhanced process yields and straightforward scalability [20,35].

2. Materials and Methods

2.1. HC device and processes

Figure 1 shows the experimental device implementing the HC-based process, including a closed hydraulic loop (total volume capacity around 230 L) and a centrifugal pump (7.5 kW nominal

Peer-reviewed version available at Processes 2019, 7, 581; doi:10.3390/pr7090581

mechanical power, rotation speed 2900 rpm). The processes were carried out at atmospheric pressure (open plant).

Such device was used in past studies to carry out innovative beer-brewing [32,33,36,37], for which application an industrial-level plant (2,000 L) was developed [38], the enhancement of biochar properties [39], and the solvent-free extraction of bioactive compounds, namely polyphenols and flavonoids, from the leaves of silver fir plants [34]. The geometry of the Venturi-shaped cavitation reactor was defined in a previous study [40].

Venturi-shaped cavitation reactors were shown to outperform other reactors based on fixed constrictions, such as orifice plates, in the treatment of viscous food liquids [35]. This superiority holds especially with liquids containing solid particles, as well as for the inactivation of spoilage microorganisms [40], and for the creation of oil-in-water stable nanoemulsions [41], all these features being relevant to the processes under study.

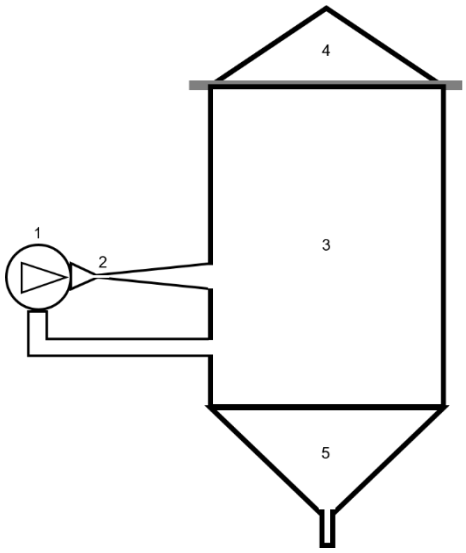

Figure 1. Experimental HC-based installation. 1 – centrifugal pump, 2 – HC reactor, 3 – main vessel, 4 – cover, 5 – discharge.

In case of a fixed mechanical constriction, such as the Venturi-shaped HC reactor shown in Figure 1, the liquid velocity and static pressure are regulated by the Bernoulli's equation [22], *i.e.*, the conservation of the mechanical energy for a moving fluid, represented in Equation (1):

$$P_1 + \rho v_1^2/2 + \rho g h_1 = P_2 + \rho v_2^2/2 + \rho g h_2 \quad (1)$$

where P_1 and P_2 (Nm^{-2}) are the upstream pressure, and the pressure at the nozzle, respectively, ρ (kgm^{-3}) is the liquid density, v_1 and v_2 (ms^{-1}) are the fluid speed upstream and through the nozzle, respectively, h_1 and h_2 (m) are the heights of the fluid, and g (ms^{-2}) is gravity. The third term at each side of Equation (1) represents the specific potential energy, while the second term represents the specific kinetic energy. Assuming equal heights, the pressure drop ($P_2 < P_1$) at the reactor's nozzle arises because of the fluid acceleration due to mass conservation ($v_2 > v_1$). Whenever P_2 drops below the vapor pressure, at a certain temperature level, local evaporation occurs, and vapor bubbles are generated.

Theoretical and experimental evidence has grown about the unique physical (mechanical and thermal) phenomena occurring at the scale of the collapsing cavitation bubbles [22,23], and the chemical phenomena such as water splitting and generation of powerful oxidants (*e.g.*, OH· hydroxyl radicals) [23,26]. However, the concentration of oxidizing compounds, which could be harmful in food processes, was found to be quite limited in the absence of specific oxidizing additives [42,43].

Despite the inherent complexity of the physico-chemical processes associated to cavitation, for fixed constrictions, a widely used dimensionless quantity, named cavitation number (σ) and derived

from the Bernoulli's equation, can be used to characterize the cavitation intensity in a flow system, in terms of easily measurable physical quantities. Its representativeness holds in most of relatively simple HC reactors, such as Venturi tubes and orifice plates [22], and relate it with the cavitational intensity, with cavitation generally arising for $\sigma < 1$.The main metric of HC processes, i.e., the cavitation number (σ), was defined long ago [44]. It is a dimensionless parameter, derived from Bernoulli's equation, and representing the ratio between the pressure drop needed to achieve vaporization, and the specific kinetic energy at the cavitation inception section, as per Equation (2):

$$\sigma = (P_0 - P_v) / (0.5 \cdot \rho \cdot v_2^2) \quad (2)$$

where P_0 (Nm^{-2}) is the average recovered pressure downstream of a cavitation reactor, such as a Venturi tube or an orifice plate, where cavitation bubbles collapse. Since the fluid was not pressurized, P_0 was assumed equal to the atmospheric pressure. P_v (Nm^{-2}) is the liquid vapor pressure, as a function of the average temperature for any given liquid. As in Equation (1), v_2 (ms^{-1}) is the flow velocity through the nozzle of the cavitation reactor, depending on the pump's inlet pressure. In this study, the values of the cavitation number during the processes were computed according to the available data, such as temperature and pump discharge; the latter were retrieved based on the consumed power, as explained in a previous study [32].

Under conditions which are easily achievable with Venturi-shaped reactors, it was found that developed cavitation, with frequent and violent bubble collapses, occurs within the range $0.1 < \sigma < 1$, and even at greater values in the presence of solid particles or dissolved gases [45,46]. In general, the lower the cavitation number, the more efficient are the cavitation processes, at least down to the onset of chocked cavitation conditions (supercavitation), even though that regime has been shown to be very efficient for disinfection purposes [47].

2.2. Orange waste samples and tests

Two HC-based extraction tests were performed with WOP, both based on organic fruits of *Citrus sinensis* (L.) Osbeck variety 'Washington navel orange', originating from Sicily, Italy. The first test (WOP1) was carried out in March 2017, with WOP from red oranges kindly provided by Ortogel S.p.A. (Caltagirone, Sicily, Italy) representing the wastes from the orange juice production line. The test WOP1 was aimed at the extraction and analysis of pectin, as well as at the analysis of the biochemical methane potential of the solid residues resulting from the process.

The second test (WOP2) was carried out in April 2019, with raw material consisting of peels manually discarded from oranges collected at a local organic farm in Ribera, Sicily, Italy. The latter test was aimed at analyzing the extraction rate of bioactive compounds such as polyphenols and EOs (terpenes).

In both tests, the WOP was immediately frozen after collection, ground in ice (maximum linear size of 10 mm), in order to avoid the degradation of bioactive compounds, then pitched into the HC device and processed in tap water only. Table 1 shows the basic features of both tests.

Table 1. Basic features of the WOP extraction tests. The WOP mass is expressed in kg of fresh weight.

Test (ID)	Water volume (L)	WOP mass (kg)	Test duration (min)	Temperature (°C)
WOP1	120	42	270	14.5 – 96
WOP2	147	6.38	127	18.5 – 80

In both tests, the HC device was not airtight, allowing volatile compounds to escape, thereby hindering the retaining of terpenes in the aqueous solutions and affecting the EO yield extraction results. Among monoterpenes, *d*-limonene is particularly volatile; for example, its fraction, extracted from hops during high temperatures steps of the brewing process, could not be retained in finished beer [48,49].

The evolution of the temperature and the cavitation number are shown in Figure 2a for the test WOP1 and in Figure 2b for the test WOP2, along with the respective sampling points. No

temperature control (*i.e.*, no cooling step) was performed, thus the overall heating was the result of the balance between the mechanical energy supplied by the pump's impeller and the heat loss from the uninsulated device [36].

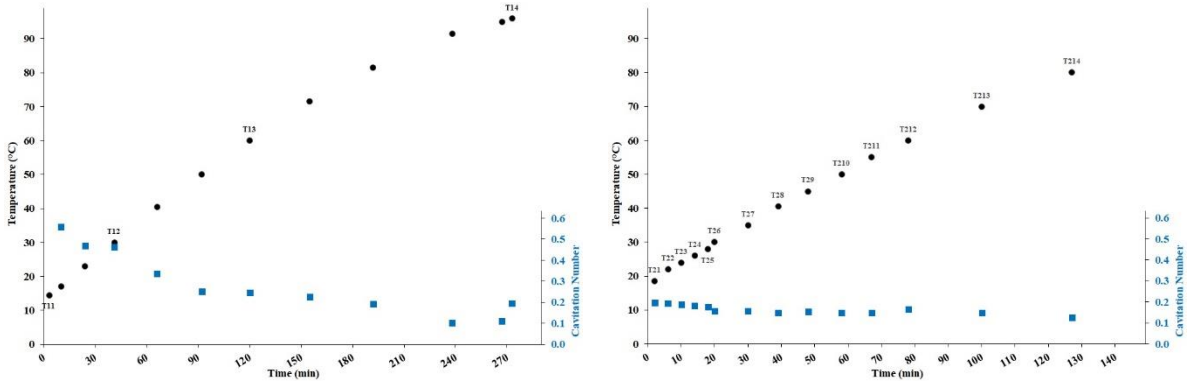

(**a**) (**b**)

Figure 2. Evolution of the temperature and the cavitation number, along with sampling points (from T11 to T14 for WOP1 and from T21 to T214 for WOP2), in the two tests: (**a**) WOP1; (**b**) WOP2.

In the earlier phase of the test WOP1 (more than 30 min), the cavitation number was rather high (0.46 to 0.57), pointing to relatively poor cavitation performance. This behavior derived from the centrifugal pump running in a suboptimal regime (low consumed power), and was likely due to the high concentration of the raw material (28.6% w/v). Later on, as the cavitation process caused the reduction of WOP particle size, as well as promoted the extraction and solubilization of bioproducts, the cavitation number slowly decreased, down to 0.1 at 91°C (235 min). The final increase of σ up to 0.19 was instead due to the strong friction induced by the high temperature, reducing the pump discharge and counteracting the effect of the increased vapor pressure.

Due to the suboptimal performance during the earlier phase of the test WOP1, a substantially lower concentration of WOP was used for the test WOP2 (4.3% w/v), where the sampling was much more frequent in time. Indeed, in the test WOP2, the cavitation number was as low as 0.2 from the beginning, slowly decreasing in the first 20 min, then stabilizing around 0.15, and finally decreasing again, down to 0.12, during heating from 70°C to 80°C as a result of the increasing vapor pressure. These levels of the cavitation number fell within the recommended range, found for brewing applications using the same device as in this study [32].

The specific energy consumed (electricity per kg of fresh WOP), limited to the range 18 to 80°C, was on average 0.065 kWh/kg for a heating of 10°C in WOP1, and 0.36 kWh/kg for a heating of 10°C in WOP2. This outcome is the result of the greater water volume by 1.225 times, and the lower content of raw material by 6.6 times in WOP2. However, the ratio of the specific energies (about 5.5) was lower than expected based on the above-mentioned data, because the pump in WOP2 was more efficient (higher consumed power, by 1.2 times on average), thus the heating rate was higher and the heat loss from the uninsulated device was lower. The overall consumed specific energy at the end of the WOP1 and WOP2 tests was around 0.62 kWh/kg and 2.20 kWh/kg, respectively.

2.3. Experimental and analytical procedures

2.3.1. Biochemical methane generation potential

The biochemical methane potential (BMP) of the solid residues obtained in both tests was evaluated by assays performed according to a standard method [50]. In detail, vessel-shape, static reactors of 100 mL volume were filled with a mixture consisting of a portion of the solid residues from the process of WOP1 test, and a substrate drawn from an existing biogas generation plant. The latter included mesophilic bacteria, and biomass having the following characteristics: moisture 94.2%, ash 25.1%, volatile substance (VS) 69.1%, carbon content 41.7%, hydrogen content 5.1%,

nitrogen content 2.3%, sulfur content 0.5%. One vessel contained only such substrate ("blank test"). The mass of both WOP1 process residues and the above-mentioned substrate was 0.6 g.

The vessels were kept in a thermal bath at the temperature of 38°C, and the biogas volume produced every day was measured, for 36 days, starting within 15 days after the WOP1 test. Each measurement was performed in triplicate. The contribution of the WOP to the biogas production, normalized to the content of the volatile substance, was estimated subtracting the average production of the blank test from the average production of the WOP-containing vessels.

Based on the composition of each sample, the theoretical biomethane generation potential (Th_BMP), and the theoretical relative content of methane in the biogas, were computed according to the Buswell's formulas [51]. By means of the simple multiplication of the biogas generation by the methane content, the cumulated BMP attributed to the solid residues of the test WOP1 could be assessed on a daily basis.

2.3.2. Pectin

Pectin extracted from citrus fruits is generally a high molecular weight (80−400 kDa) block copolymer alternating linear homopolymeric (poly-α(1−4)-D-galacturonic acid) and branched (poly-α(1−2)-L-rhamnosyl-α(1−4)-D-galacturonosyl with side branches of either α-L-arabinofuranose and α-D-galactopyranose) repeating units [52]. These repeating domains, schematically illustrated in Figure 3, are known as homogalacturonan (HG) and rhamnogalacturonan-I (RG-I) regions and their relative proportions determine the flexibility and rheological properties of the polymer in aqueous solution: HG regions promote molecular interactions, allowing the formation of hydrogels, while RG regions promote the formation of entangled structures, enhancing the gels' stability [53].

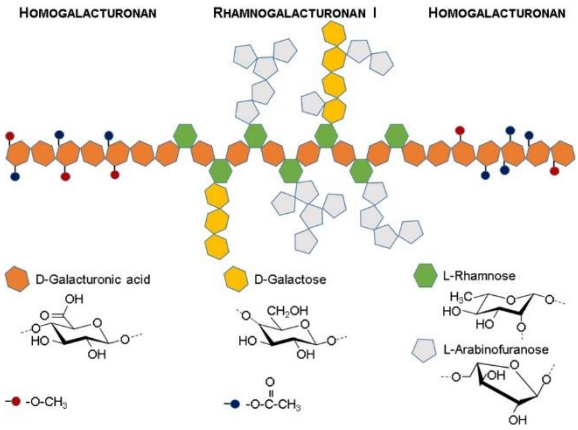

Figure 3. Schematic model of citrus fruits' pectin block copolymer structure, illustrating its two major components: homogalacturonan and rhamnogalacturonan I.

Some of the homopolymeric galacturonic acid backbone C-2, C-3 and C-5 carboxyl groups may be partially esterified with methoxyl and/or acetyl groups, or exist as uronic acid salt, affecting the polymer charge in solution [54]. The degree of esterification of pectin (proportion of methoxyl content, DE) determines the gelling mechanism, since it influences the availability of COO^- groups in solution [55]. Typically, pectin with low DE (<50%) tends to promote the presence of charged groups and form gels electrostatically stabilized by metal cations [54], making it particularly appropriate for food and beverage, pharmaceutical and nutraceutical applications, because it does not require sugar or acidic conditions to gel [56].

Only the aqueous sample labeled as T14 in Figure 2(a) displaying the WOP1 test, extracted at the end of the process (temperature of 96°C), was analyzed in quadruplicate. The analysis of the respective extracted pectin content was carried out 18 months after the test. During this period, the

samples of lyophilized pectin, consisting of a pale orange powder with a delicate fragrance, was kept at room temperature in sealed plastic vessels.

The structure of the respective subsamples, labeled as P2, P3, P4, and P5, was characterized by means of diffuse reflectance infrared Fourier transform (DRIFT) spectroscopy, using a Bruker Vertex 70 FTIR spectrometer equipped with a wide band MCT detector and a Specac selector, in the range 4000 to 500 cm^{-1}, at 4 cm^{-1} resolution.

The spectra were the result of ratioing 500 co-added single beam scans for each sample, *i.e.*, grinded pectin powder (Figure 4) diluted in grinded FTIR grade KBr, in the appropriate proportion to assure the validity of the Kubelka-Munk assumptions [57], against the same number of scans for the background (grinded KBr). The spectra were transformed to Kubelka-Munk units using OPUSTM software (Bruker Optics, Germany) and further processed using ORIGIN™ software (OriginLab Corporation, USA).

Figure 4. Sample of lyophilized pectin powder from the WOP1 test (right), which was ground in a quartz mortar (left) prior to the DRIFT-IR experiments.

2.3.3. Polyphenols analysis by HPLC-DAD

After the HC process, the samples collected during the test WOP2 (from T21 to T214) were centrifuged (5 min, 9000 rpm, at 5°C). The supernatants (5 mL) were then partitioned with n-hexane (5 mL x 3) to completely remove lipophilic compounds in order to obtain the aqueous phases. The pellets (process residues) were dried in oven (40°C, for 48h), extracted (5% w/v) with ethanol 75% in a ultrasonic bath (30°C) for 30 min, similarly to the method described in [58], and partitioned with n-hexane (1:1). The same extraction method was also applied to dried peels (dry WOP). The extracts were evaporated to dryness, re-suspended in methanol and acid water (pH 2.5 by HCOOH) 50:50 (v/v) and then injected (15 µL) in a Perkin® Elmer Flexar liquid chromatograph equipped with a quaternary 200Q/410 pump and an LC 200 diode array detector (DAD) (all from Perkin Elmer®, Bradford®, CT, USA).

The stationary phase consisted in an Agilent® Zorbax® SB-18 column (250 × 4.6 mm, 5 µm), kept at 30 °C. The eluents were (A) acidified water (at pH 2.5 adjusted with HCOOH) and (B) acetonitrile/ water (90/10, at pH 2.5 adjusted with HCOOH) and the following gradient was applied: 0–20 min (5 – 20% B), 20–22 min (20% B), 22–32 min (20 – 25% B), 32–42 min (25 – 100% B), 42-43 min (100 – 5% B), with an elution flow of 0.6 mL/min.

The quantification of different polyphenols was performed through an external standard method, using stock solutions of the following compounds: caffeic acid, naringin and hesperidin (all from Sigma-Aldrich, Milan, Italy). The identification of single compounds was done on the basis of their UV-VIS spectra and the comparison with literature [58]. All solvents used for the analyses were purchased from Sigma-Aldrich (Milan, Italy). All measurements were performed in triplicate.

2.3.4. Analysis of terpenes

After the WOP2 test, the terpenes analyses were performed on all the aqueous phase samples (from T21 to T214) and on five selected solid residue samples (T21, T22, T26, T210 and T214). Moreover, the analyses were also carried out on raw orange peel samples stored at -20° C.

Liquid extraction was done by mixing 1 mL of aqueous phase samples with the same volume of heptane containing 20 ppm tridecane as an internal standard [59], in 2 ml glass vials with a Teflon-coated screw cap (Perkin-Elmer, Norwalk, CT, USA).

The solid residue samples were dehydrated on filter paper with a vacuum pump for 5 min and 0.5 mg of FW for each sample were closed in glass vial and suspended in 2 mL of heptane with 20 ppm tridecane and small amount of sodium chloride, stirred for 5 min at room temperature. This procedure was also applied to raw orange peel samples previously grounded in liquid nitrogen in a mortar to a fine powder (0.5 mg FW).

All samples were incubated in an ultrasonic bath for 30 min at 0°C and then slowly stirred for 24 h at room temperature. The supernatant (100 µL) was used for analysis after centrifugation at 4000 rpm for 10 min at room temperature in an Eppendorf centrifuge mod. 5810R (Westbury, NY, USA). The heptane extracts (1 µL) were analyzed using an Agilent 7820A gas chromatograph (GC) interfaced to an Agilent 5977E mass spectrometer (MS) with EI ionization and single quadrupole mass analyzer (Agilent Tech., Palo Alto, CA, USA). A chromatographic column Agilent HP-INNOWax capillary 50 m, 0.20 mm, ID 0.4 µm DF was used. The GC injection temperature was 250°C, splitless mode, and the oven was programmed at 40°C for 1 min, followed by a ramp of 5°C/min to 200°C, and of 10°C/min to 260°C. This high temperature was held for 5 min.

The identification of terpene compounds was based on both peak matching with library spectral database (NIST 11), and Kovats retention indices (KRI) retrieved in the literature for the identified compounds. All the measurements were performed in triplicate and the amount of each terpene was expressed as percentage of total terpenes.

3. Results

3.1. Biochemical methane generation potential

Table 2 shows the composition of the solid residues from the samples collected during the test WOP1, in terms of the relative contents of moisture, ash, volatile substance, carbon, hydrogen, nitrogen, and sulfur. As well, the Th_BMP, and the theoretical methane (CH_4) relative content in the biogas, are shown.

Table 2. Composition of solid residues from the samples of the WOP1 test. Unless specified otherwise, units are % w/w on dry basis.

Sample	Moisture [1]	Ash	VS	C	H	N	S	Th_BMP [2]	CH_4 [3]
T11	95.6	3.8	96.2	42.7	6.2	0.7	0.1	421.3	50.0
T12	96.6	3.5	96.5	42.2	6.3	0.7	0.1	415.6	49.6
T13	97.0	3.2	96.8	42.6	6.2	0.9	0.1	408.9	48.9
T14	96.6	2.8	97.2	41.1	6.4	0.7	0.1	392.5	49.3

[1] Unit: % w/w as determined. [2] Unit: mL/g VS. [3] Unit: % in biogas.

Figure 5 shows the cumulated biogas generation, in unit of mL, from all the samples on a daily basis, including the blank sample, as resulting from the average of the triplicate measurements. At the end of the 36-days period, the biogas generation achieved the levels of 185, 554, 564, 637, and 763 mL, for the blank, T11, T12, T13, and T14 samples, respectively. The standard deviations of the measurements did not exceed 3% of the respective average value at the 8th day and afterwards (for example, 497 ± 14 mL for the sample T14 at the 8th day), thus visible differences were also statistically significant.

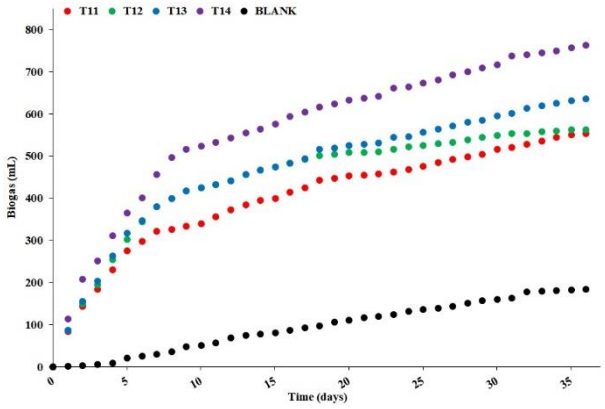

Figure 5. Cumulated biogas generation from all the WOP1 test samples, including the blank sample.

Most of the biogas generation from the sample T11 to T14 occurred within the first 7-8 days (57 to 68% of the overall generation), while it was delayed, and evolving much more linearly with time, from the blank sample. In particular, it arises that the substantial part of the biogas generation from the samples T11 to T14, after the first week, was due to the emissions from the substrate constituting the blank sample.

After the subtraction of the biogas generation from the blank sample, and the conversion to methane, based on the relative content of CH_4 in the biogas (as shown in Table 2), the BMP attributed to the solid residues of the samples, extracted during the WOP1 test, could be calculated. Figure 6 shows the assessed cumulated methane generation, in unit of mL per gram of volatile substance, from the sample T11 to T14, on a daily basis. At the end of the 36-days period, the methane generation rates achieved the levels of 256, 261, 318, and 763 mL/g VS, for the samples T11, T12, T13, and T14, respectively.

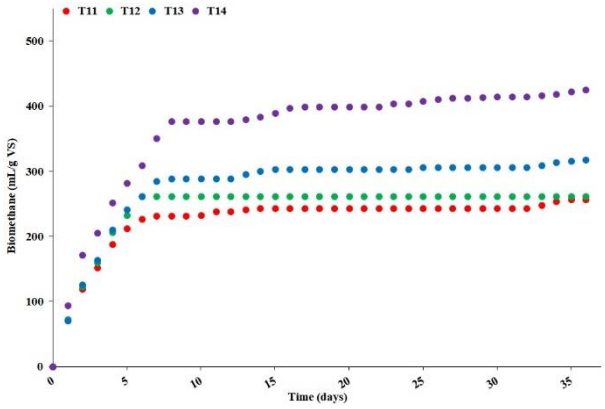

Figure 6. Cumulated methane generation from all the WOP1 test samples, after subtraction of the generation from the blank sample.

Almost all the methane was generated within the first 7-8 days, from 88% for sample T14, to 100% for sample T12. After 36 days, the actual BMP was -39%, -37%, -22%, and +8% of the Th_BMP shown in Table 2, for the samples T11, T12, T13, and T14, respectively. Thus, the HC process was able to increase effectively the methane generation from the solid residues of the WOP material, with a clearly increasing trend during the hydrocavitation process, up to the full exploitation of the respective BMP.

Considering the chemical energy density of the methane at the level of 10.5 kWh/m^3, the data shown in Table 2, and the above-mentioned methane generation rates at the end of the 36-days period, Table 3 shows the energy balance of the process for the four analyzed samples. However, the electricity and the methane chemical energy cannot be directly compared. In particular, the

consumed electricity should be converted into the chemical energy of methane used for power generation, with conversion factors depending on the specific generation technology.

Table 3. Energy balance of the process: consumed specific energy (electricity, during the HC process) and specific energy available in the generated methane (chemical energy). Units are kWh/kg fresh weight.

Sample	Consumed specific energy	Specific Energy in the generated methane
T11	0.01	0.28
T12	0.09	0.28
T13	0.27	0.34
T14	0.62	0.45

3.2. Pectin

Pectin isolated from four subsamples (P2, P3, P4 and P5) by lyophilization of sample T14, collected at the end of the WOP1 test (Figure 2(a)) was analyzed via DRIFT spectroscopy. Figure 7 shows the corresponding DRIFT spectra (2000-500 cm^{-1} region), which exhibit the typical features of pectin.

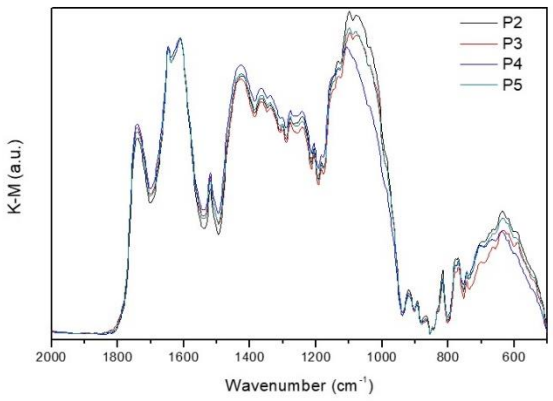

Figure 7. DRIFT spectra of the pectin samples in the 2000-500 cm^{-1} region, normalized to the $\nu_{as}COO^-$ band carboxylate groups, at 1610 cm^{-1}.

The strong bands in the 1800-1550 cm-1 region, with maxima at 1740, 1647 and 1610 cm-1, are assigned to the stretching modes of carbonyl groups from esterified galacturonic acid ($\nu C{=}O_{ester}$) and non-esterified hydrogenated acidic carbonyl groups ($\nu C{=}O_{acid}$), and of carboxylate groups ($\nu_{as}COO^-$), respectively [6]. The 1550-1200 cm^{-1} region is dominated by CH_x and C-O-H deformation modes, partially overlapped with ester related stretching modes [60,61], and include:

- The $\delta_{as}CH_3$ and δ_sCH_3 (from ester methyl groups in the galacturonic rings and rhamnose rings of the pectin backbone) at 1520 and 1365 cm^{-1};
- The ν_sCOO^- at ~1425 cm^{-1};
- The $\nu C\text{-}O\text{-}C_{ester}$ at 1277cm^{-1};
- The $\delta_{ip}C\text{-}O\text{-}H$ (from alcohol hydroxyl groups in the pyranose rings of the pectin chain) at 1242 cm^{-1}.

The 1200-950 cm^{-1} region contains a set of very intense bands partially overlapped typical of pectin, assigned to skeletal (νC-C) and C-O-C stretching (νC-O-C) modes of the pyranose rings and of the glycosidic bonds, and to a combination of the νC-OH and νC-C modes from the pyranose rings [62,63]. Finally, the 950-500 cm-1 region contains the bands related to the external deformation vibrations of methyl, methylene and methyne groups (ρCH_x and δC-H) [61].

The degree of esterification of pectin (percent of esterified carboxyl groups) was obtained by spectral analysis of the 1800-1550 cm^{-1} region, as the ratio of ester carboxyl to total carboxyl peak areas, as shown in Equation (3) [64]:

$$DE = \Sigma A_{\nu C=O ester} / (\Sigma A_{\nu C=O ester} + A_{\nu C=O acid} + A_{\nu as COO^-}) \quad (3)$$

The νC=O and $\nu_{as}COO^-$ band areas of the samples were estimated by decomposing the 1900-850 cm^{-1} region (two consecutive absorption zeros) into a sum of Gaussian components, using a nonlinear least-squares fitting [6].

The components' centers, full width at half maxima and integrated areas are summarized in Table 4 for the four samples. Based on these results, it was possible to determine a very low degree of esterification for this pectin, namely 17.05 ± 0.60%.

Table 4. Decomposition results of the 1800-1550 cm^{-1} region of the DRIFT spectra: Centers (C), full width at half maxima (FWHM) and integrated areas (A) of the νC=O and $\nu_{as}COO^-$ band areas

Sample (ID)	Band areas	C (cm^{-1})	FWHM (cm^{-1})	A (a.u.)	DE
P2	$\nu C=O_{ester}$	1741	47	28.03	0.1786
	$\nu C=O_{acid}$	1648	18	3.37	
	$\nu_{as}COO^-$	1608	137	125.50	
P3	$\nu C=O_{ester}$	1740	50	28.67	0.1715
	$\nu C=O_{acid}$	1649	19	3.04	
	$\nu_{as}COO^-$	1609	143	135.42	
P4	$\nu C=O_{ester}$	1741	48	28.66	0.1664
	$\nu C=O_{acid}$	1648	18	3.05	
	$\nu_{as}COO^-$	1610	148	140.55	
P5	$\nu C=O_{ester}$	1741	47	28.55	0.1655
	$\nu C=O_{acid}$	1648	19	3.09	
	$\nu_{as}COO^-$	1610	149	140.87	

3.3. Polyphenols

As an example, Figure 8 shows the chromatograms of the sample T28 (39 min, 40.5°C), its pellet (process residues), and the dry WOP. As expected, the flavanones naringin and hesperidin dominated the chromatogram of the dry WOP, along with another peak, labeled as F5 and classified as an unidentified flavanone derivative, according to its UV spectra. The same peaks dominated the chromatogram of the pellet, although the relative contribution of naringin was lower.

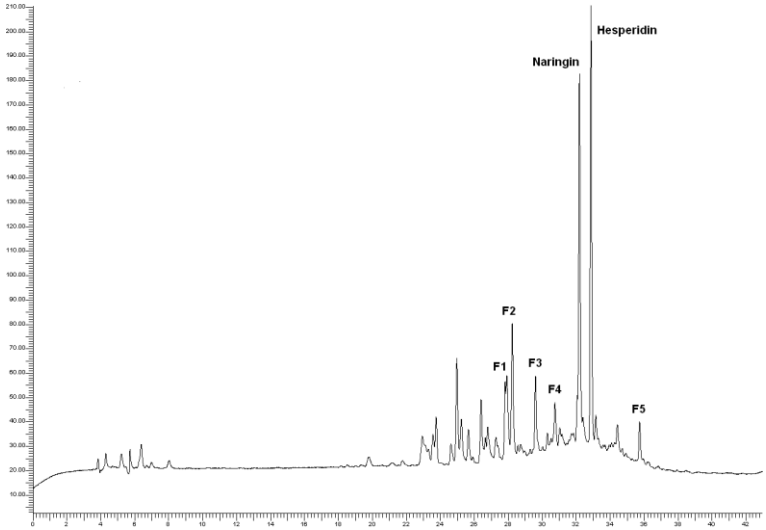

(**a**)

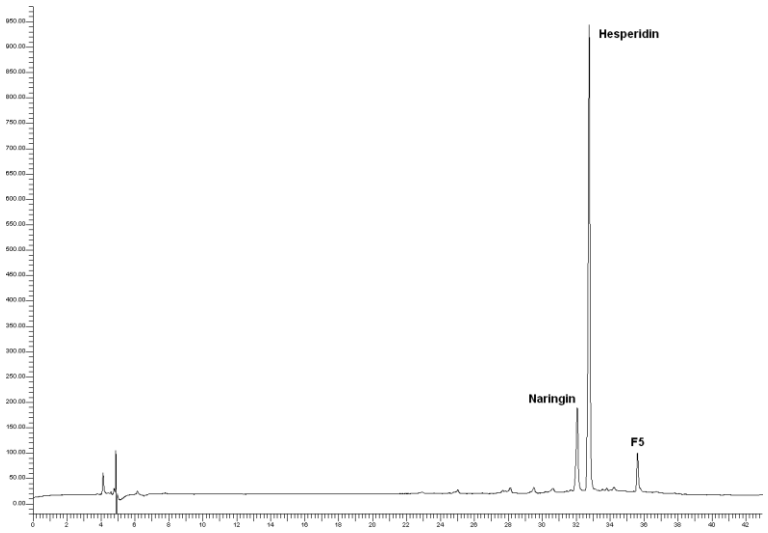

(**b**)

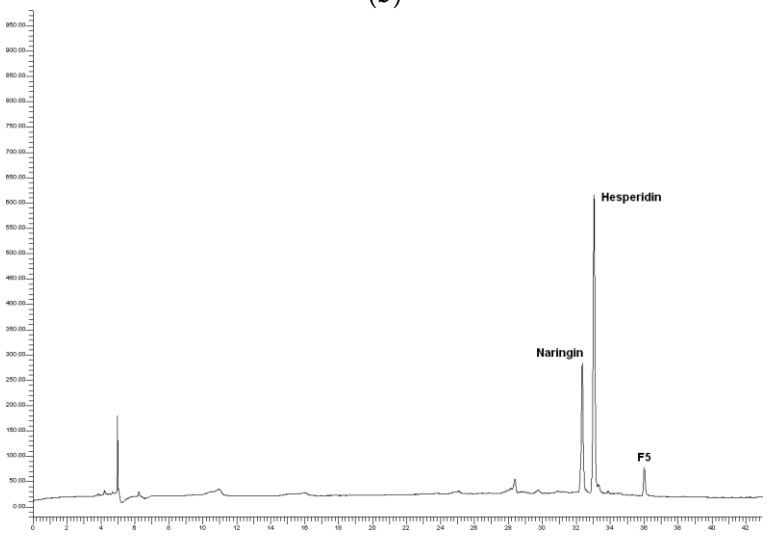

(**c**)

Figure 8. Chromatograms of polyphenols for the sample T28 of the test WOP2: (**a**) aqueous phase; (**b**) process residues; (**c**) dry WOP.

In the aqueous phase, along with the same peaks attributed to naringin and hesperidin, the peaks labeled as F1 to F4 were detected and identified as flavanones derivatives based on their UV spectra. The unlabeled peaks were putatively identified as hydroxycinnamic acid derivatives (HAD), based on their UV spectra similar to those of caffeic acid, with peak absorbance around 330 nm, instead of 280 nm as for flavanones [65].

Figure 9 shows the total polyphenolic content (flavanones and HAD) present in the aqueous phase of the whole system (total volume = 147 L). The sample T27 (30 min, 37°C) showed significantly lower total polyphenols than all the samples from T22 to T214 ($p < 0.05$). Moreover, the total polyphenolic content of the sample T23 was significantly higher than sample T28 ($p < 0.05$).

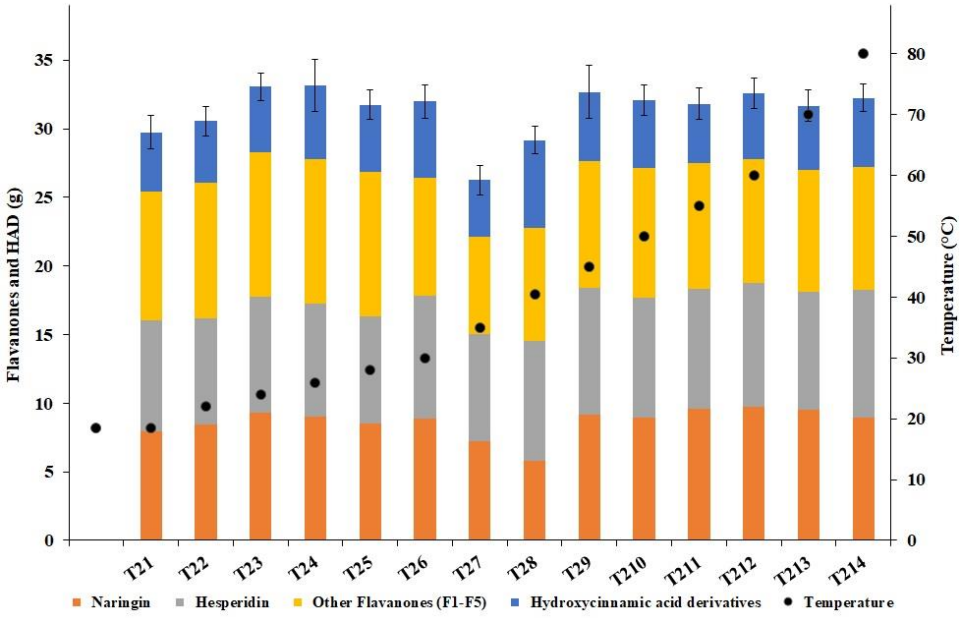

Figure 9. Content of Flavanones and Hydroxycinnamic acid derivatives in the aqueous phase.

Quite surprisingly, the higher content of polyphenols, mostly due to the increase of naringin and other flavanones (F1-F5), was reached after 10 min of the beginning of the process time (sample T23, temperature of 24°C), corresponding to about 30 passes of the entire volume of the processed mixture through the cavitation reactor. Moreover, the apparent stability of the total content up to the sample T26 (20 min, 30°C), and the following rather abrupt decrease at T27 (30 min, 35°C), in turn followed by the return to the levels typical of T23-T26, could suggest a possible kinetics involving thermal degradation and further extraction from the circulating WOP.

The total contents of naringin, hesperidin, and other flavanones (F1-F5) in the raw fresh WOP (6.379 kg) were 16.39, 36.26, and 2.95 g, respectively. Based on these data, and the total contents (including HAD) observed in the aqueous phase (Figure 9), the extraction yields peaked in correspondence of the samples T23 (59.5%) and T24 (59.6%). However, the extraction yield was already as high as 53.5% at T21, *i.e.*, after just 2 min of process time and about 6 passes of the entire volume of the processed mixture through the cavitation reactor.

3.4. Terpenes

Figure 10 shows the concentration of the detected monoterpenes in the aqueous phase and in the solid residues, derived from the observed concentration in each of the samples collected during the test WOP2. In the aqueous phase (Figure 10(a), unit ng/mL), *d*-limonene represented more than 73% of all monoterpenes in any of the first seven samples and, in particular, more than 93% in sample T22. In the solid residues (Figure 10(b), unit ng/g fresh weight, except for *d*-limonene, expressed in unit μg/g fresh weight), *d*-limonene represents more than 96% of all monoterpenes in any sample.

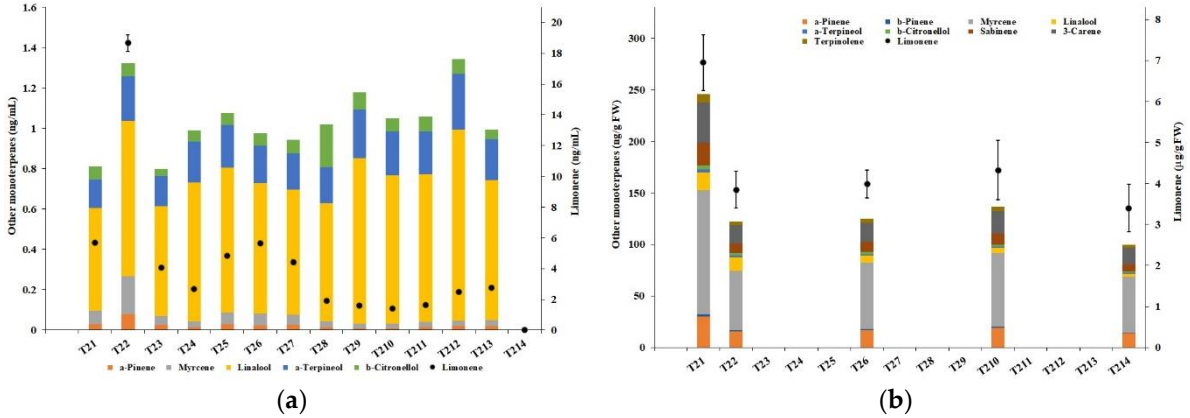

Figure 10. Concentration of monoterpenes: (**a**) aqueous phase; (**b**) solid residues.

The concentration of *d*-limonene in the aqueous solution more than doubled from the sample T21 (2 min, 18.5°C) to T22 (6 min, 22°C); such pattern was shared by the other detected monoterpenes, although with milder changes. As mentioned in Section 2.2, volatile compounds were free to escape from the processing device, which explains why the limonene concentration decreased abruptly by almost 80% from the sample T22 to T23 (10 min, 24°C). Since then on, the concentration of *d*-limonene stabilized around similar levels, eventually further decreasing from sample T28 (39 min, 40.5°C) onwards, reaching zero in the last sample T214 (127 min, 80°C), along with all the other terpenes. Beyond cavitation, temperature looks like to play an important role in the volatilization of the terpenes.

The fast and effective extraction of *d*-limonene from the WOP was confirmed by the abrupt decrease of its concentration (by about 45%) in the solid residues, from the sample T21 to sample T22, again stabilizing around similar levels onwards. It should also be noted that the mass of solid residues decreased substantially during the HC-based process (as noted visually). Hence, the respective actual content of *d*-limonene probably decreased much more than represented in Figure 10(b).

In the raw WOP, limonene accounted for over 96% of all monoterpenes, with a concentration of 5.9 ± 0.9 µg/g FW. Based on the original WOP mass (fresh weight) of 6.379 kg, the total content of *d*-limonene in the raw material can be estimated at the level of 38 ± 6 mg. The peak concentration in the aqueous phase (sample T22) was 18.7 ± 0.5 ng/mL, which, multiplied by the volume of the water (147 L), translates into a total content of 2.75 ± 0.07 mg, *i.e.*, a yield just over 7%. However, it is unknown how much terpene escaped the hydrocavitation open reactor during the first 6 min of the process, as well as data concerning the solid residues suggest that the extraction yield was actually much higher, at least 45% and likely substantially higher.

Finally, it is interesting to notice that, among the other detected monoterpenes, myrcene was the most relatively abundant in the solid residues, while linalool prevailed in the aqueous solution, in full agreement with the alcohol nature of the latter.

4. Discussion

The device, used to process the orange peel waste, making no use of proprietary components, is easy to construct and maintain, and its operation at the pre-industrial scale was proven by the experiments carried out at the real scale (more than 100 L of water, processed WOP raw material of about 6.4 and 42 kg). On the other hand, the scalability of the proposed device, up to the industrial scale (1,700 L), was recently demonstrated in the brewing sector [66].

The hydrodynamic cavitation processes, sustained by means of a circular Venturi-shaped reactor, were able to effectively and fully separate and extract the most valued components of waste orange peel. It is remarkable that no solvents or any additives, other than tap water, were used in the extraction processes.

As shown in Section 3.1, the biomethane generation potential was boosted, in terms of both total cumulated production, and generation rate. Within only 3 min of process time, corresponding to less than 10 passes of the entire volume of the processed mixture through the cavitation reactor, at the temperature of 14.5°C, the BMP was already at the level of 61% of its theoretical value. As well, the specific energy content of the generated methane (chemical energy) was about 30 times higher than the specific consumed energy (electricity). Since then, the BMP increased up to the Th_BMP at the end of the process WOP1 (273 min, temperature of 96°C), but the energy balance became negative.

From the point of view of the energy balance, it would be imperative to limit the process time as much as possible, *i.e.*, to few min. However, the process time should be optimized based on the assessment of the overall value of all the extractable materials, such as pectin, polyphenols and terpenes, as well as on the use of the substrate resulting after the anaerobic digestion (*e.g.*, disposal, composting, etc.). Such topics are recommended for further research.

Due to the apparent suboptimal cavitation regime during most of the WOP1 process, especially during the first 60-90 min, it is likely that simple technical adjustments, such as a different centrifugal pump, could produce even better results. However, with a lower concentration of WOP in the aqueous mixture, as in the test WOP2, the HC process was carried out in the optimal regime, as proven by the low levels of the cavitation number. Thus, it is expected that an optimized HC process will lead to higher methane generation in a shorter process time also for higher WOP concentrations.

According to the results presented in Section 3.2, the pectin isolated in the sample collected at the end of the process WOP1 showed a very low degree of esterification, namely $17.05 \pm 0.60\%$, meaning that it would be particularly appropriate for food and beverage, pharmaceutical and nutraceutical applications, because it does not require sugar or acidic conditions to form stabilized gels. It should be noted that this result nicely agrees with previous studies in which pectin from WOP originating from red oranges from the same area of Sicily, extracted via microwave hydrodistillation and gravity, was shown to have a DE of 25%, suggesting that the pectin from the red orange pulp is likely to have a very low DE [67].

We remind that WOP (exo-, meso-, and endocarp) contains not only the outer skin (exocarp), and the peel (exo- and mesocarp), but also endocarp residues. It is remarkable that, as mentioned in Section 2.3.2., pectin, analyzed 18 months after extraction and lyophilization, remained stable during prolonged storage at room temperature in direct contact with air's oxygen. Actually, after another three months in the same plastic vessel, the same pectin continues to show no sign of degradation, pointing to the stabilization effect of powerful antioxidant orange biophenols including flavanones (Section 3.3) clearly found in the WOP2 aqueous solutions, and likely available in even greater concentration in the sample T14 from the test WOP1.

Overall, the test WOP1 proved that the HC process allowed the effective extraction of high-quality pectin from the waste orange peel, and a very efficient exploitation of the biomethane generation potential from the solid residues of the process. As well, no microbiological degradation or spoilage was detected in the liquid sample T14, even though it is unlikely that any relevant concentration of antimicrobial *d*-limonene was retained in the aqueous solution, due to the very high working temperature (as shown for sample T214 from the test WOP2). We hypothesize that the reason for the apparent microbiological stability, lies in the well-known effective disinfection carried out by the HC-thermal process [40].

As shown in Section 3.3, water-soluble flavanones naringin and hesperidin constituted by far the greatest part of polyphenols in the WOP. Both compounds were extracted in the aqueous solution quite effectively and efficiently by means of the HC process, and partially transformed into other compounds, mostly other flavanones, and likely in hydroxycinnamic acid derivatives. Overall, the extraction process yield was assessed at the level of nearly 60%, with regard to the sum of the detected compounds. Such yield was achieved within 10 min of process time, and after just 2 min the yield was at the level of about 53%, thus proving the effectiveness of the extraction.

We hypothesize that the other flavanones (peaks F1 to F4 in Figure 8) might have derived from hesperidin and/or naringin, following the loss of at least one hexose unit. In their turn, since these peaks were practically undetectable in the chromatogram of the process residues, this decomposition could have been due to cavitation processes occurring in the liquid phase. In addition, the peaks shown just on the left of the peak F1 region in the chromatogram for the aqueous phase (Figure 8, unlabeled peaks), attributed to HAD, were not observed in dry WOP or process residues, and could be considered as a distinct effect of the cavitation process.

From the decrease of the *d*-limonene concentration in the solid residues (Section 3.4), a lower limit of 45% for the respective extraction yield in the aqueous phase was inferred, such compound being by far the most abundant monoterpene in the WOP. However, the actual extraction yield is expected to be actually much higher, as suggested by two evidences. First, the abrupt drop of its concentration in the aqueous phase shortly after its highest value (6 min of process time), pointing to its fast volatilization. Second, the mass loss from the solid residues due to the continuous extraction, leading to the overestimation of the respective total content of *d*-limonene based on its concentration. In forthcoming practical applications, airtight HC extractors will be used in order to retain liquid limonene, both floating and emulsified in the aqueous solution due to the emulsifying action of pectin [15].

The high volatility of orange peel EOs under environmental conditions (in particular, of *d*-limonene, that is chemically unstable) hinders their effectivity as flavorings in the food industry (affecting the shelf-life), and as biopesticides in agronomic applications [68]. Moreover, the antimicrobial action of *d*-limonene was found to markedly increase when applied as an oil-in-water nanoemulsion, for example reducing the thermal resistance of *Listeria monocytogenes* by one hundred times, against only two to five times when added directly [69].

Therefore, methods have been proposed to reduce the volatility, to increase the stability, and to control the release of such compounds. Two recent studies proposed the nanoencapsulation of orange peel EOs [70], and *d*-limonene [71], respectively, in oil-in-water nanoemulsions created by means of ultrasonic irradiation (acoustic cavitation), and stabilized with a mixture of pectin and whey proteins. Thus, the combination of cavitation processes and pectin appears very promising for the retention and effectivity of *d*-limonene, provided that its volatilization is prevented.

Indeed, the residual retention of *d*-limonene in the aqueous solution, up to the sample T27 (30 min, 35°C) in the WOP2 test (Figure 10(a)), could have been favored by two factors. First, the likely micronization and at least partial emulsification of the terpenes in water, based on the well-established effectivity of HC processes in the creation of stable sub-micron oil-in-water emulsions [41,72]. Second, the effectivity of pectin as an emulsifying compound, as well as a stabilizer for emulsions [17]. Due to the effective extraction of high-quality pectin in the aqueous phase (Section 3.2), the micronized Limonene drops could have been partly emulsified and stabilized, concurring to the limitation of its volatilization. Further research will investigate these relevant emulsion chemistry aspects.

Finally, further research using optimized devices and processes, will allow the rigorous, quantitative comparison of the proposed process with either conventional or newer extraction techniques. As an example, the effective retaining and recovery of orange peel oil during the HC process will allow the determination of comprehensive performance indices, such as those recently advanced, based on the extraction yield, the energy efficiency and the quality of the product [73].

5. Conclusions

This study reports remarkable results concerning the valorization of waste orange peel via controlled hydrodynamic cavitation. One of the strengths is the presentation of outcomes on the semi-industrial scale, such as the extraction from 42 kg of WOP with 120 L of tap water (test WOP1). This allowed proving the scalability of the process, which often remains an open issue with laboratory reports dealing with the extraction of valued bioproducts from (at most) a few hundred grams of a biological matrix.

Although the extraction conditions were far from being optimal under various aspects, both water-soluble flavanones and *d*-limonene, by far the most abundant monoterpene in red orange and Washington Navel orange EO, were extracted within 10 min of process time and at room temperature. High-quality (low degree of esterification and high molecular weight) pectin was easily isolated from the aqueous extract via straightforward lyophilization. The cellulose- and hemicellulose-rich solid residue showed excellent methane generation potential under anaerobic digestion, with few min of process time enough to result in a very high ratio of the energy contained in the generated methane to the consumed energy.

The results shown in this study open the route to the integral valorization of WOP via a simple, low cost and highly effective technology and the related method, requiring water as the unique additional raw material. The relevance of the presented findings also arises from the abundance of the WOP (around 25 MT/year as a by-product of the agrifood industry), the likely applicability to the by-products of the processing of other citrus fruits, and the rapid spreading of the controlled HC processes in several food-related productions [27,28,34].

The process applied in this study adheres to the six principles of green extraction [74], even though wide margins for further improvement, based on thorough optimization, clearly exist.

Author Contributions: Conceptualization, FRANCESCO MENEGUZZO, CECILIA BRUNETTI, LORENZO ALBANESE, FEDERICA ZABINI and MARIO PAGLIARO; Data curation, FRANCESCO MENEGUZZO, CECILIA BRUNETTI, ALEXANDRA FIDALGO, ROSARIA CIRIMINNA, LORENZO ALBANESE, ANTONELLA GORI, LUANA BEATRIZ DOS SANTOS NASCIMENTO and ANNA DE CARLO; Formal analysis, FRANCESCO MENEGUZZO and MARIO PAGLIARO; Funding acquisition, FRANCESCO MENEGUZZO, RICCARDO DELISI, FRANCESCO FERRINI and MARIO PAGLIARO; Investigation, FRANCESCO MENEGUZZO, CECILIA BRUNETTI, ROSARIA CIRIMINNA, RICCARDO DELISI, LORENZO ALBANESE, ANNA DE CARLO and MARIO PAGLIARO; Methodology, FRANCESCO MENEGUZZO, CECILIA BRUNETTI, ALEXANDRA FIDALGO, ROSARIA CIRIMINNA, RICCARDO DELISI, LORENZO ALBANESE, ANTONELLA GORI, LUANA BEATRIZ DOS SANTOS NASCIMENTO, ANNA DE CARLO and LAURA M. ILHARCO; Resources, FRANCESCO MENEGUZZO, RICCARDO DELISI and MARIO PAGLIARO; Software, CECILIA BRUNETTI, ALEXANDRA FIDALGO, ANTONELLA GORI, LUANA BEATRIZ DOS SANTOS NASCIMENTO and ANNA DE CARLO; Supervision, FRANCESCO MENEGUZZO, FRANCESCO FERRINI and MARIO PAGLIARO; Validation, FRANCESCO MENEGUZZO, CECILIA BRUNETTI, ANNA DE CARLO and LAURA M. ILHARCO; Visualization, FRANCESCO MENEGUZZO, CECILIA BRUNETTI, ALEXANDRA FIDALGO, ANTONELLA GORI and ANNA DE CARLO; Writing – original draft, FRANCESCO MENEGUZZO and FEDERICA ZABINI; Writing – review & editing, FRANCESCO MENEGUZZO, CECILIA BRUNETTI, ALEXANDRA FIDALGO, FEDERICA ZABINI, FRANCESCO FERRINI, LAURA M. ILHARCO and MARIO PAGLIARO.

Funding: This research received no external funding.

Acknowledgments: The authors gratefully acknowledge Dr. Mauro Centritto (CNR-IPSP) for the continuous support and very important suggestions.

Conflicts of Interest: The authors declare no conflict of interest.

References

1. Satari, B.; Karimi, K. Citrus processing wastes: Environmental impacts, recent advances, and future perspectives in total valorization. *Resour. Conserv. Recycl.* **2018**, *129*, 153–167, doi:10.1016/j.resconrec.2017.10.032.

2. USDA Citrus: World Markets and Trade. *United States Dep. Agric. Foreign Agric. Serv.* **2019**, *July*, 1–11, doi:10.1016/S1097-8690(11)70006-3.

3. Negro, V.; Ruggeri, B.; Fino, D.; Tonini, D. Life cycle assessment of orange peel waste management. *Resour. Conserv. Recycl.* **2017**, *127*, 148–158, doi:10.1016/j.resconrec.2017.08.014.

4. Boukroufa, M.; Boutekedjiret, C.; Petigny, L.; Rakotomanomana, N.; Chemat, F. Bio-refinery of orange peels waste: A new concept based on integrated green and solvent free extraction processes using ultrasound and microwave techniques to obtain essential oil, polyphenols and pectin. *Ultrason. Sonochem.* **2015**, *24*, 72–79, doi:10.1016/j.ultsonch.2014.11.015.

5. Hilali, S.; Fabiano-Tixier, A. S.; Ruiz, K.; Hejjaj, A.; Ait Nouh, F.; Idlimam, A.; Bily, A.; Mandi, L.; Chemat, F. Green extraction of essential oils, polyphenols and pectins from orange peel employing solar energy. Towards a Zero-Waste Biorefinery. *ACS Sustain. Chem. Eng.* **2019**, acssuschemeng.9b02281, doi:10.1021/acssuschemeng.9b02281.

6. Fidalgo, A.; Ciriminna, R.; Carnaroglio, D.; Tamburino, A.; Cravotto, G.; Grillo, G.; Ilharco, L. M.; Pagliaro, M. Eco-Friendly Extraction of Pectin and Essential Oils from Orange and Lemon Peels. *ACS Sustain. Chem. Eng.* **2016**, *4*, 2243–2251, doi:10.1021/acssuschemeng.5b01716.

7. Ciriminna, R.; Fidalgo, A.; Delisi, R.; Carnaroglio, D.; Grillo, G.; Cravotto, G.; Tamburino, A.; Ilharco, L. M.; Pagliaro, M. High-Quality Essential Oils Extracted by an Eco-Friendly Process from Different Citrus Fruits and Fruit Regions. *ACS Sustain. Chem. Eng.* **2017**, *5*, 5578–5587, doi:10.1021/acssuschemeng.7b01046.

8. Pourbafrani, M.; Forgács, G.; Horváth, I. S.; Niklasson, C.; Taherzadeh, M. J. Production of biofuels, limonene and pectin from citrus wastes. *Bioresour. Technol.* **2010**, *101*, 4246–4250, doi:10.1016/j.biortech.2010.01.077.

9. Ciriminna, R.; Lomeli-Rodriguez, M.; Demma Carà, P.; Lopez-Sanchez, J. A.; Pagliaro, M. Limonene: a versatile chemical of the bioeconomy. *Chem. Commun.* **2014**, *50*, 15288–96, doi:10.1039/c4cc06147k.

10. Singh, G.; Upadhyay, R. K.; Narayanan, C. S.; Padmkumari, K. P.; Rao, G. P. Chemical and fungitoxic investigations on the essential oil of Citrus sinensis (L.) Pers. *J. Plant Dis. Prot.* 1993, *100*, 69–74.

11. Hollingsworth, R. G. Limonene, a Citrus Extract, for Control of Mealybugs and Scale Insects. *J. Econ. Entomol.* **2005**, *98*, 772–779, doi:10.1603/0022-0493-98.3.772.

12. Keinan, E.; Alt, A.; Amir, G.; Bentur, L.; Bibi, H.; Shoseyov, D. Natural ozone scavenger prevents asthma in sensitized rats. *Bioorganic Med. Chem.* **2005**, *13*, 557–562, doi:10.1016/j.bmc.2004.09.057.

13. Fitzgerald, C.; Hossain, M.; Rai, D. K. Waste/By-Product Utilisations. In *Innovative Technologies in Beverage Processing*; Aguiló-Aguayoi, I., Plaza, L., Eds.; John Wiley & Sons, Ltd: Chichester, UK, 2017; pp. 297–309.

14. Pagliaro, M.; Rosaria, C.; Fidalgo, A. M. A.; Delisi, R.; Ilharco, L. Pectin production and global market. *Agro Food Ind. Hi Tech* **2016**, *27*, 17–20.

15. Ciriminna, R.; Chavarría-Hernández, N.; Inés Rodríguez Hernández, A.; Pagliaro, M. Pectin: A new perspective from the biorefinery standpoint. *Biofuels, Bioprod. Biorefining* **2015**, *9*, 368–377, doi:10.1002/bbb.1551.

16. Leroux, J.; Langendorff, V.; Schick, G.; Vaishnav, V.; Mazoyer, J. Emulsion stabilizing properties of

pectin. *Food Hydrocoll.* **2003**, *17*, 455–462, doi:10.1016/S0268-005X(03)00027-4.

17. Dickinson, E. Hydrocolloids acting as emulsifying agents – How do they do it? *Food Hydrocoll.* **2018**, *78*, 2–14, doi:10.1016/j.foodhyd.2017.01.025.

18. Fernandez, M. E.; Ledesma, B.; Román, S.; Bonelli, P. R.; Cukierman, A. L. Development and characterization of activated hydrochars from orange peels as potential adsorbents for emerging organic contaminants. *Bioresour. Technol.* **2015**, *183*, 221–228, doi:10.1016/j.biortech.2015.02.035.

19. Lam, S. S.; Liew, R. K.; Lim, X. Y.; Ani, F. N.; Jusoh, A. Fruit waste as feedstock for recovery by pyrolysis technique. *Int. Biodeterior. Biodegrad.* **2016**, *113*, 325–333, doi:10.1016/j.ibiod.2016.02.021.

20. Holkar, C. R.; Jadhav, A. J.; Pinjari, D. V.; Pandit, A. B. Cavitationally Driven Transformations: A Technique of Process Intensification. *Ind. Eng. Chem. Res.* **2019**, acs.iecr.8b04524, doi:10.1021/acs.iecr.8b04524.

21. Gogate, P. R.; Pandit, A. B. Hydrodynamic cavitation reactors: a state of the art review. *Rev. Chem. Eng.* **2001**, *17*, 1–85, doi:10.1515/REVCE.2001.17.1.1.

22. Pawar, S. K.; Mahulkar, A. V.; Pandit, A. B.; Roy, K.; Moholkar, V. S. Sonochemical effect induced by hydrodynamic cavitation: Comparison of venturi/orifice flow geometries. *AIChE J.* **2017**, *63*, 4705–4716, doi:10.1002/aic.15812.

23. Yasui, K.; Tuziuti, T.; Sivakumar, M.; Iida, Y. Sonoluminescence. *Appl. Spectrosc. Rev.* **2004**, *39*, 399–436, doi:10.1081/ASR-200030202.

24. Dindar, E. An Overview of the Application of Hydrodinamic Cavitation for the Intensification of Wastewater Treatment Applications: A Review. *Innov. Energy Res.* **2016**, *5*, 1–7, doi:10.4172/ier.1000137.

25. Doltade, S. B.; Dastane, G. G.; Jadhav, N. L.; Pandit, A. B.; Pinjari, D. V.; Somkuwar, N.; Paswan, R. Hydrodynamic cavitation as an imperative technology for the treatment of petroleum refinery effluent. *J. Water Process Eng.* **2019**, *29*, 100768, doi:10.1016/j.jwpe.2019.02.008.

26. Ciriminna, R.; Albanese, L.; Meneguzzo, F.; Pagliaro, M. Wastewater remediation via controlled hydrocavitation. *Environ. Rev.* **2017**, *25*, 175–183, doi:10.1139/er-2016-0064.

27. Carpenter, J.; Badve, M.; Rajoriya, S.; George, S.; Saharan, V. K.; Pandit, A. B. Hydrodynamic cavitation: an emerging technology for the intensification of various chemical and physical processes in a chemical process industry. *Rev. Chem. Eng.* **2017**, *33*, 433–468, doi:10.1515/revce-2016-0032.

28. Panda, D.; Manickam, S. Cavitation Technology—The Future of Greener Extraction Method: A Review on the Extraction of Natural Products and Process Intensification Mechanism and Perspectives. *Appl. Sci.* **2019**, *9*, 766, doi:10.3390/app9040766.

29. Cravotto, G.; Mariatti, F.; Gunjevic, V.; Secondo, M.; Villa, M.; Parolin, J.; Cavaglià, G. Pilot Scale Cavitational Reactors and Other Enabling Technologies to Design the Industrial Recovery of Polyphenols from Agro-Food By-Products, a Technical and Economical Overview. *Foods* **2018**, *7*, 130,

doi:10.3390/foods7090130.

30. Sarvothaman, V. P.; Simpson, A. T.; Ranade, V. V. Modelling of vortex based hydrodynamic cavitation reactors. *Chem. Eng. J.* **2018**, doi:10.1016/j.cej.2018.08.025.

31. Asaithambi, N.; Singha, P.; Dwivedi, M.; Singh, S. K. Hydrodynamic cavitation and its application in food and beverage industry: A review. *J. Food Process Eng.* **2019**, e13144, doi:10.1111/jfpe.13144.

32. Albanese, L.; Ciriminna, R.; Meneguzzo, F.; Pagliaro, M. Beer-brewing powered by controlled hydrodynamic cavitation: Theory and real-scale experiments. *J. Clean. Prod.* **2017**, *142*, 1457–1470, doi:10.1016/j.jclepro.2016.11.162.

33. Albanese, L.; Ciriminna, R.; Meneguzzo, F.; Pagliaro, M. Innovative beer-brewing of typical, old and healthy wheat varieties to boost their spreading. *J. Clean. Prod.* **2018**, *171*, 297–311, doi:10.1016/j.jclepro.2017.10.027.

34. Albanese, L.; Bonetti, A.; D'Acqui, L. P.; Meneguzzo, F.; Zabini, F. Affordable Production of Antioxidant Aqueous Solutions by Hydrodynamic Cavitation Processing of Silver Fir (Abies Alba Mill.) Needles. *Foods* **2019**, *8*, 65, doi:10.3390/foods8020065.

35. Albanese, L.; Meneguzzo, F. 10 - Hydrodynamic Cavitation Technologies: A Pathway to More Sustainable, Healthier Beverages, and Food Supply Chains. In *Processing and Sustainability of Beverages*; Grumezescu, A. M., Holban, A. M., Eds.; Woodhead Publishing, 2019; pp. 319–372 ISBN 978-0-12-815259-1.

36. Ciriminna, R.; Albanese, L.; Di Stefano, V.; Delisi, R.; Avellone, G.; Meneguzzo, F.; Pagliaro, M. Beer produced via hydrodynamic cavitation retains higher amounts of xanthohumol and other hops prenylflavonoids. *LWT - Food Sci. Technol.* **2018**, *91*, 160–167, doi:10.1016/j.lwt.2018.01.037.

37. Albanese, L.; Ciriminna, R.; Meneguzzo, F.; Pagliaro, M. Gluten reduction in beer by hydrodynamic cavitation assisted brewing of barley malts. *LWT - Food Sci. Technol.* **2017**, *82*, 342–353, doi:10.1016/j.lwt.2017.04.060.

38. CAVIBEER | CNR & Bysea S.r.l. Cavibeer Available online: http://www.cavibeer.com/ (accessed on Jul 25, 2019).

39. Albanese, L.; Baronti, S.; Liguori, F.; Meneguzzo, F.; Barbaro, P.; Vaccari, F. P. Hydrodynamic cavitation as an energy efficient process to increase biochar surface area and porosity: A case study. *J. Clean. Prod.* **2019**, *210*, 159–169, doi:10.1016/J.JCLEPRO.2018.10.341.

40. Albanese, L.; Ciriminna, R.; Meneguzzo, F.; Pagliaro, M. Energy efficient inactivation of Saccharomyces cerevisiae via controlled hydrodynamic cavitation. *Energy Sci. Eng.* **2015**, *3*, 221–238, doi:10.1002/ese3.62.

41. Carpenter, J.; George, S.; Saharan, V. K. Low pressure hydrodynamic cavitating device for producing highly stable oil in water emulsion: Effect of geometry and cavitation number. *Chem. Eng. Process. Process Intensif.* **2017**, *116*, 97–104, doi:10.1016/j.cep.2017.02.013.

42. Ciriminna, R.; Albanese, L.; Meneguzzo, F.; Pagliaro, M. Hydrogen Peroxide: A Key Chemical for Today's Sustainable Development. *ChemSusChem* **2016**, *9*, 3374–3381, doi:10.1002/cssc.201600895.

43. Yusaf, T.; Al-Juboori, R. A. Alternative methods of microorganism disruption for agricultural applications. *Appl. Energy* **2014**, *114*, 909–923, doi:10.1016/j.apenergy.2013.08.085.

44. Yan, Y.; Thorpe, R. B. Flow regime transitions due to cavitation in the flow through an orifice. *Int. J. Multiph. Flow* **1990**, *16*, 1023–1045, doi:10.1016/0301-9322(90)90105-R.

45. Bagal, M. V; Gogate, P. R. Wastewater treatment using hybrid treatment schemes based on cavitation and Fenton chemistry: a review. *Ultrason. Sonochem.* **2014**, *21*, 1–14, doi:10.1016/j.ultsonch.2013.07.009.

46. Gogate, P. R. Cavitation: an auxiliary technique in wastewater treatment schemes. *Adv. Environ. Res.* **2002**, *6*, 335–358, doi:10.1016/S1093-0191(01)00067-3.

47. Šarc, A.; Kosel, J.; Stopar, D.; Oder, M.; Dular, M. Removal of bacteria Legionella pneumophila , Escherichia coli, and Bacillus subtilis by (super)cavitation. *Ultrason. Sonochem.* **2018**, *42*, 228–236, doi:10.1016/j.ultsonch.2017.11.004.

48. King, A. J.; Dickinson, J. R. Biotransformation of hop aroma terpenoids by ale and lager yeasts. *FEMS Yeast Res.* **2003**, *3*, 53–62, doi:10.1016/S1567-1356(02)00141-1.

49. Dickinson, J. R. Terpenoids in Beer. In *Beer in Health and Disease Prevention*; Preedy, V. R., Ed.; Academic Press: San Diego, CA (USA), 2009; pp. 327–332 ISBN 9780123738912.

50. Angelidaki, I.; Alves, M.; Bolzonella, D.; Borzacconi, L.; Campos, J. L.; Guwy, A. J.; Kalyuzhnyi, S.; Jenicek, P.; Van Lier, J. B. Defining the biomethane potential (BMP) of solid organic wastes and energy crops: A proposed protocol for batch assays. *Water Sci. Technol.* **2009**, *59*, 927–934, doi:10.2166/wst.2009.040.

51. Buswell, A. M.; Mueller, H. F. Mechanism of Methane Fermentation. *Ind. Eng. Chem.* **1952**, *44*, 550–552, doi:10.1021/ie50507a033.

52. Mohnen, D. Pectin structure and biosynthesis. *Curr. Opin. Plant Biol.* **2008**, *11*, 266–277, doi:10.1016/j.pbi.2008.03.006.

53. Morra, M.; Cassinelli, C.; Cascardo, G.; Nagel, M. D.; Della Volpe, C.; Siboni, S.; Maniglio, D.; Brugnara, M.; Ceccone, G.; Schols, H. A.; Ulvskov, P. Effects on interfacial properties and cell adhesion of surface modification by pectic hairy regions. *Biomacromolecules* **2004**, *5*, 2094–2104, doi:10.1021/bm049834q.

54. Morris, G. A.; Foster, T. J.; Harding, S. E. The effect of the degree of esterification on the hydrodynamic properties of citrus pectin. *Food Hydrocoll.* **2000**, *14*, 227–235, doi:10.1016/S0268-005X(00)00007-2.

55. McConaughy, S. D.; Stroud, P. A.; Boudreaux, B.; Hester, R. D.; McCormick, C. L. Structural characterization and solution properties of a galacturonate polysaccharide derived from Aloe vera capable of in situ gelation. *Biomacromolecules* **2008**, *9*, 472–480, doi:10.1021/bm7009653.

56. Zhao, S.; Yang, F.; Liu, Y.; Sun, D.; Xiu, Z.; Ma, X.; Zhang, Y.; Sun, G. Study of chemical characteristics, gelation properties and biological application of calcium pectate prepared using apple or citrus pectin. *Int. J. Biol. Macromol.* **2018**, *109*, 180–187, doi:10.1016/j.ijbiomac.2017.12.082.

57. Yang, L.; Kruse, B. Revised Kubelka–Munk theory I Theory and application. *J. Opt. Soc. Am. A* **2004**, *21*, 1933, doi:10.1364/JOSAA.21.001933.

58. Khan, M. K.; Abert-Vian, M.; Fabiano-Tixier, A. S.; Dangles, O.; Chemat, F. Ultrasound-assisted extraction of polyphenols (flavanone glycosides) from orange (Citrus sinensis L.) peel. *Food Chem.* **2010**, *119*, 851–858, doi:10.1016/j.foodchem.2009.08.046.

59. Raffa, K. F.; Smalley, E. B. Interaction of pre-attack and induced monoterpene concentrations in host conifer defense against bark beetle-fungal complexes. *Oecologia* **1995**, *102*, 285–295, doi:10.1007/BF00329795.

60. Filippov, M. P. IR spectra of pectin films. *J. Appl. Spectrosc.* **1974**, *17*, 1052–1054, doi:10.1007/BF00635158.

61. Synytsya, A.; Čopíková, J.; Matějka, P.; Machovič, V. Fourier transform Raman and infrared spectroscopy of pectins. *Carbohydr. Polym.* **2003**, *54*, 97–106, doi:10.1016/S0144-8617(03)00158-9.

62. Chatjigakis, A. K.; Pappas, C.; Proxenia, N.; Kalantzi, O.; Rodis, P.; Polissiou, M. FT-IR spectroscopic determination of the degree of esterification of cell wall pectins from stored peaches and correlation to textural changes. *Carbohydr. Polym.* **1998**, *37*, 395–408, doi:10.1016/S0144-8617(98)00057-5.

63. Assifaoui, A.; Loupiac, C.; Chambin, O.; Cayot, P. Structure of calcium and zinc pectinate films investigated by FTIR spectroscopy. *Carbohydr. Res.* **2010**, *345*, 929–933, doi:10.1016/j.carres.2010.02.015.

64. Monsoor, M. A.; Kalapathy, U.; Proctor, A. Improved method for determination of pectin degree of esterification by diffuse reflectance Fourier transform infrared spectroscopy. *J. Agric. Food Chem.* **2001**, *49*, 2756–2760, doi:10.1021/jf0009448.

65. Nkhili, E.; Tomao, V.; El Hajji, H.; El Boustani, E. S.; Chemat, F.; Dangles, O. Microwave-assisted water extraction of green tea polyphenols. *Phytochem. Anal.* **2009**, *20*, 408–415, doi:10.1002/pca.1141.

66. Albanese, L.; Meneguzzo, F. 7 - Hydrodynamic Cavitation-Assisted Processing of Vegetable Beverages: Review and the Case of Beer-Brewing. In *Production and Management of Beverages*; Grumezescu, A. M., Holban, A. M., Eds.; Woodhead Publishing, 2019; pp. 211–257 ISBN 978-0-12-815260-7.

67. Ciriminna, R.; Fidalgo, A.; Delisi, R.; Tamburino, A.; Carnaroglio, D.; Cravotto, G.; Ilharco, L. M.; Pagliaro, M. Controlling the Degree of Esterification of Citrus Pectin for Demanding Applications by Selection of the Source. *ACS Omega* **2017**, *2*, 7991–7995, doi:10.1021/acsomega.7b01109.

68. Ciriminna, R.; Meneguzzo, F.; Pagliaro, M. Orange Oil. In *Green Pesticides Handbook: Essential Oils for Pest Control*; Nollet, L. M. L., Rathore, H. S., Eds.; CRC Press: Boca Raton FL, 2017; pp. 291–303 ISBN 978-1-49-875938-0.

69. Maté, J.; Periago, P. M.; Palop, A. When nanoemulsified, d-limonene reduces Listeria monocytogenes

heat resistance about one hundred times. *Food Control* **2016**, *59*, 824–828, doi:10.1016/j.foodcont.2015.07.020.

70. Ghasemi, S.; Jafari, S. M.; Assadpour, E.; Khomeiri, M. Production of pectin-whey protein nano-complexes as carriers of orange peel oil. *Carbohydr. Polym.* **2017**, *177*, 369–377, doi:10.1016/j.carbpol.2017.09.009.

71. Ghasemi, S.; Jafari, S. M.; Assadpour, E.; Khomeiri, M. Nanoencapsulation of D-limonene within nanocarriers produced by pectin-whey protein complexes. *Food Hydrocoll.* **2018**, *77*, 152–162, doi:10.1016/j.foodhyd.2017.09.030.

72. Wu, Z.; Tagliapietra, S.; Giraudo, A.; Martina, K.; Cravotto, G. Harnessing cavitational effects for green process intensification. *Ultrason. Sonochem.* **2019**, *52*, 530–546, doi:10.1016/j.ultsonch.2018.12.032.

73. Razzaghi, S. E.; Arabhosseini, A.; Turk, M.; Soubrat, T.; Cendres, A.; Kianmehr, M. H.; Perino, S.; Chemat, F. Operational efficiencies of six microwave based extraction methods for orange peel oil. *J. Food Eng.* **2019**, *241*, 26–32, doi:10.1016/j.jfoodeng.2018.07.018.

74. Chemat, F.; Vian, M. A.; Cravotto, G. Green extraction of natural products: Concept and principles. *Int. J. Mol. Sci.* **2012**, *13*, 8615–8627, doi:10.3390/ijms13078615.